Modeling and construction of an Electromagnetic Suspension System based on a discrete PID controller

J. D. Ríos[a], A. A. Velásquez[a]

[a] *Applied Electromagnetism Group, Universidad EAFIT*
Medellín, Colombia

Abstract

This paper presents the design and construction of a magnetic levitation system of a ferromagnetic sphere. The magnetic levitation is achieved with the electromagnetic and dynamic analysis of the system which is used to implement a digital PID controller. The PID controller is designed with pole assignment technique in the analog domain and converted to the digital domain with a sample time small enough to stabilize the system. The magnetic suspension system parameters were obtained carefully in order to achieve a good starting model as near as possible to the real system.The global structure of the hardware system is presented. Infrared sensors were used to sense the position of the sphere, a microcontroller PIC18F2550 with an analog to digital converter of 10 bits was used to sample the voltage position signal as well as to implement the digital PID controller. The control signal was used to activate a MOSFET's gate which controlled the average voltage through the coil. Finally, in order to test the performance of the system, spheres and bodies with different dimension, mass, geometry and material were put in suspension successfully which demonstrated the robustness of the designed controller.

Keywords: Magnetic levitation, Digital PID control, Electromagnetism, CAD tools

1. Introduction

From several decades ago magnetic levitation has been a demonstration of great visual impact to illustrate the potential use of levitation in applications focused on industry, trade, transportation, medicine or entertainment. For example, in electrical engineering are found applications associated with the modeling of dynamic systems [1], control of unstable systems [2], low friction bearings [3], artificial pumps used to substitute the heart [4], magnetic traps for fluids with diamagnetic properties such as liquid Helium [5], levitation of microrobots in

Email addresses: jriosrui@eafit.edu.co (J. D. Ríos), avelas26@eafit.edu.co (A. A. Velásquez)

three dimensions [6] and transportation systems, like the high speed Maglev train [7].

The EMS (Electromagnetic Suspension) is one of the most unstable dynamical systems and highly non-linear due to the nature of the phenomenon and to the Earnshaw's theorem, which stated that no stationary object made of magnets in a fixed configuration can held in stable equilibrium by any combination of static magnetic or gravitational forces [8].For this reason, during decades this system has been an ideal platform for working researchers, in which the goal is to implement classical and modern control techniques, always making use of emerging technologies in the fields of electronic instrumentation and new materials. In this context the system has a high value as an educational tool. This paper deals with the modelation from the first principles of an electromagnetic suspension system, showing the tuning of the controller PID parameters by the Routh-Hurwithz criterion and CAD tools, optimization of the transient response of the system and finally, the controller's real implementation through a digital system. The paper also tries to show how the integration of different areas such as basic science and engineering can help to obtain optimal and effective solutions to real problems.

2. Magnetic Suspension System

The main components of the Electromagnetic Suspension System are presented in Fig. 1. In the system a solid ferromagnetic sphere levitates by means of a magnetic force which opposes to its weight. The sphere position is sensed optically with a couple of infrared emitter-receptor.

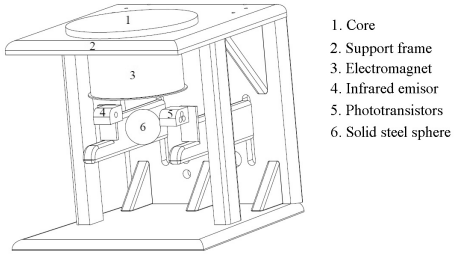

Figure 1: Components of the electromagnetic suspension system

2.1. Magnetic force

The inductance of the coil is a decreasing function of the ferromagnetic sphere position. When the sphere is removed $x \to \infty$ the inductance is L_m, and when the sphere is in contact with the coil ($x = 0$) the total inductance increases in L_s, so the total inductance is $L_m + L_s$. The variation between the two extremes can be approximated in several ways; one accurate way to do this approximation is with (1).

$$L(x) = L_m + \frac{L_s}{1 + \frac{x}{c}} \tag{1}$$

To obtain the magnetic force, we begin with the stored magnetic energy and then make use of magnetic co-energy concept [9]. The coil magnetic co-energy is given by (2).

$$W(i, x) = \frac{1}{2} L(x) i^2 \tag{2}$$

Therefore, we can obtain the magneticforce on the sphere generated by the coil like the gradient of (2), as is shown in (3).

$$f(x, i) = \frac{\partial W(i, x)}{\partial x} = -\frac{L_s c}{2} \frac{i^2}{(x + c)^2} = -K \frac{i^2}{(x + c)^2} \tag{3}$$

Where $K = \frac{L_s c}{2}$.

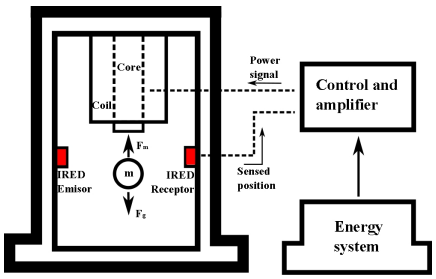

Figure 2: Scheme of the Electromagnetic Suspension System indicating the forces acting on the sphere

By means of the Newton's second law as is illustrated in the left side of Fig. 2, we can explain the movement of the ferromagnetic sphere in one dimension. The sphere has a weight which is represented by the force vector F_g . The magnetic force F_m over the sphere is generated by the coil's magnetic field. Therefore, the acceleration of the sphere can be obtainedby the Newton's second law as is shown in (4).

$$\ddot{x} = -\frac{K}{m} \frac{i^2}{(x + c)^2} + g \tag{4}$$

This is a non-linear differential equation. In order to apply linear controltechniques it is needed to linearize the equation. It can be done with decomposition of the acceleration of the sphere in Taylor series keeping only the linear terms. Doing this around $x = x_0$ and$i = i_0$, and taking in consideration only the incremental terms we obtain (5).

$$\ddot{x} = -2\frac{K}{m} \frac{i_0}{(x_0 + c)^2} i + 2\frac{K}{m} \frac{i_0^2}{(x_0 + c)^3} x \tag{5}$$

Taking Laplace transform of this linear second order differential equation we can obtain the transfer function of the coil-sphere subsystem (6).

$$\frac{X(s)}{I(s)} = \frac{\omega^2 \frac{(x_0+c)^2}{i_0}}{s^2 - \omega^2} \tag{6}$$

Where $\omega^2 = 2\frac{K}{m}\frac{i_0^2}{(x_0+c)^3}$. This is the electromechanical system transfer function which relates the coil current and sphere position. In (6) ω is the natural frequency of the plant. The relationship between the coil voltage and current can be easily obtained by analyzing the RL system which describes the electrical behavior of the coil. This is shown in Fig. 3.

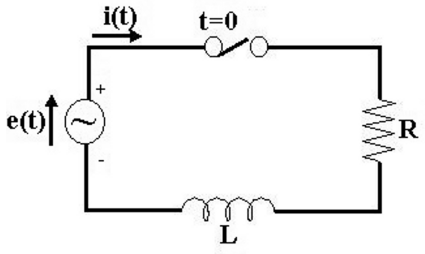

Figure 3: Electrical model of the coil circuit

Applying the voltage Kirchhoff's law we obtain (7).

$$e(t) = Ri(t) + L\frac{di(t)}{dt} \tag{7}$$

Here $e(t)$ is the voltage excitation on the system, R is the coil resistance, L its inductance and i is the current intensity. To obtain the circuit transfer function we take the Laplace transform making the entire initial conditions zero (8).

$$E(s) = RI(s) + LsI(s) \tag{8}$$

So, the transfer function is (9).

$$\frac{I(s)}{E(s)} = \frac{1}{Ls + R} \tag{9}$$

Finally, combining (6) and (9) thetransfer function of the system is obtained, as is shown in (10).

$$G(s) = \frac{X(s)}{E(s)} = \frac{\omega^2 \frac{(x_0+c)^2}{i_0}}{(s^2 - \omega^2)(R + Ls)} \tag{10}$$

This is the transfer function of a third order unstable systemwhich arises from the existence of one pole in the left halfcomplex plane.

2.2. Position sensing

The position of the sphere is sensed optically by one infrared photodiode OP293 and three infraredphototransistors OP593. The voltage produced is proportional to the sphere position, according to (11).

$$V_s = G_s x \tag{11}$$

Where G_s is the sensor gain. Therefore, the transfer function of the sensor is (12).

$$\frac{V_s(s)}{X(s)} = G_s \tag{12}$$

2.3. Power system

The power system was implemented with PWM (Pulse Width Modulation) [10]. A control signal is generated by the controller and transformed to a PWM signal which is used to cut and saturate the gate of a MOSFET producing an average voltage in the coil's terminals. The conversion from control signal to PWM and from PWM to average voltage is obtained in a linear region, so the effect is a conversion with a constant transfer function. This process is shown in Fig. 4. The conversion factor 1000/4950 has units PWM_duty/mV , where the PWM duty cycle varies in the range from 0 (0%) to 1000 (100%), according to the internal arrangement of the microcontroller's PWM module, while that the voltage control can vary from 0 mV to 4950 mV, value limited by the real feed voltage of the microcontroller.

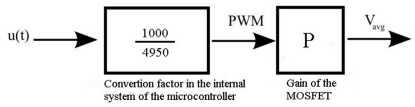

Figure 4: Conversion from control signal to average voltage

In that way the change from control signal $u(t)$ to average voltage V can be described by (13).

$$V_{avg} = \frac{1000}{4950} P u(t) \tag{13}$$

Thus, the power system transfer function is represented by (14).

$$G_p = \frac{V_{avg}(s)}{U(s)} = \frac{1000}{4950} P \tag{14}$$

2.4. Controller

The controller used in the Electromagnetic Suspension System is a digital PID controller. Its modeling was done in the continuous domain, and then was carried out to the discrete domain using a sample time small enough to model properly the real system. A PID controller produces a control signal according to three operations done on an error signal, which is the difference between the reference signal and the output signal. The proportional term (P) makes the control signal be proportional to the error signal. The integral action (I) gives a control signal according to the accumulation of error reducing the steady state error. Finally, the derivative action (D) acts on the variation of the error introducing damping in the error variation and sensibility in the controller. The general form of the PID controller is shown in (15).

$$u(t) = K_p e(t) + K_i \int_0^t e(t)dt + K_d \frac{d}{dt} e(t) \tag{15}$$

And its transfer function is shown in (16).

$$\frac{U(s)}{E(s)} = K_p + \frac{K_i}{s} + K_d s \tag{16}$$

The constants K_p ,K_i and K_d can be interpreted as a weight that assigns an escalation to the control action according to the variation of each component of the PID controller.

2.5. Control system

The control system employed in the Electromagnetic Suspension System is shown in Fig. 5.

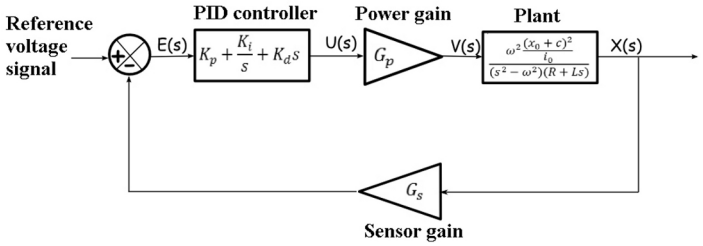

Figure 5: Block diagram of the Electromagnetic Suspension System in closed loop

The Fig. 5 and Fig. 2 can complement each other so that the whole system can be understood. The sphere position is sensed optically and converted to a voltage signal. The position signal sensed is subtracted from a reference voltage signal. In this way is obtained the error signal $e(t)$ which is mathematically manipulated by the controller to obtain a control signal $u(t)$. The control signal $u(t)$ is amplified by a power amplifier that produces an average output voltage V_{avg} which controls the sphere's position. The sphere's position is sensed, and the loop is repeated again.

3. Experimental System

In order to obtain the parameters of the Magnetic Levitation System an experiment was designed whose configuration is shown in Fig. 6.

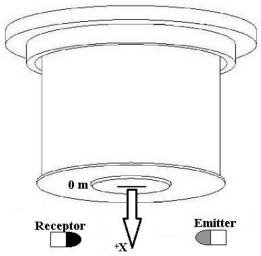

Figure 6: Experimental configuration to measure the sphere's position

The sphere position is measured from the coil's bottom which is the zero reference. Different parameters likethe position, position voltage, the current needed to attract the sphere to the coil's core given a fixed position and the PWM duty cycle were taken and related.

3.1. Parameters of the system

Table 1: Electromagnetic Suspension System parameters

Parameter	Symbol	Value
Sphere mass	m	0.0163 Kg
Gravity	g	9.764 $\frac{\mathrm{m}}{\mathrm{s}^2}$
Equilibirum sphere speed	v_0	0 $\frac{\mathrm{m}}{\mathrm{s}}$
Equilibirum sphere position	x_0	0.0116 m
Equilibirum coil current	i_0	1.03 A
Equilibirum coil voltage	u_0	7.21 V
Coil resistance	R	7 Ω
Coil inductance	L	0.0713 H

3.2. Magnetic force parameters

By using the configuration shown in Fig. 6 were taken different measures of position and the current needed to put the sphere in equilibrium for each particular position. The curve obtained is shown in Fig. 7.

As it was shown in (4), the net force acting on the sphere can be described by the Newton's second law. In the equilibrium, where magnetic and gravitational forces are equal, the net acceleration is zero, as is shown in (17).

$$0 = g - \frac{K}{m}\frac{i^2}{(x+c)^2} \tag{17}$$

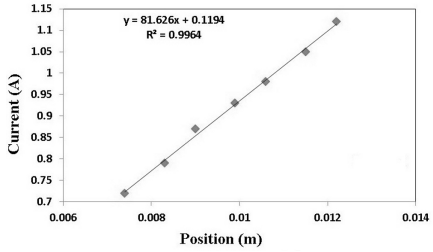

Figure 7: Curve of Position (m) vs Current (A)

In this way, by expressing the current i in function of the position x, we obtain (18).

$$i = \sqrt{\frac{mg}{K}}x + \sqrt{\frac{mg}{K}}c \tag{18}$$

So, if we can obtain a linear relation between the current i and the equilibrium position x, it is possible to find the magnetic force's parameters K and c with (18). This linear relation is evident in Fig. 7 (the correlation parameter R is near to 1). The parameters K and c were obtained through a linear regression giving the results shown in (19) and (20).

$$K = \frac{mg}{p^2} \tag{19}$$

$$c = \frac{b}{\sqrt{\frac{mg}{K}}} \tag{20}$$

Magnetic force is then expressed in (21), with units given in Newtons (N).

$$f(x,i) = -0.00002385365425\frac{i^2}{(x+0.001463235294)^2} \tag{21}$$

3.3. Sensed position

From the zero reference, several measures of position were taken with their respective position voltage given by the sensors. The curve obtained is shown in Fig. 8.

In Fig. 8 we can see two linear regions suitable to implement a linear controller. It was chosen the region for position values between 0.0104 m and 0.0117 m. The sensor gain in the equilibrium sphere position x_0 is given in (22).

$$G_s = -1900\frac{\mathrm{V}}{\mathrm{m}} \tag{22}$$

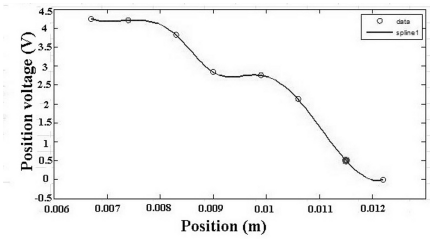

Figure 8: Position voltage given by the IRED sensors (V) vs Position (m)

3.4. Power system

As it was shown in (14), we can express the power gain like the product of a constant value ($\frac{1000}{4950}$) which is the conversion factor within the microcontroller and the value P which is the transfer function between the coil's average voltage and the PWM duty cycle in the MOSFET's gate. Different measures of the average voltage obtained in the coil's terminals were taken for different PWM duty cycles applied on the MOSFET's gate. The most linear region was obtained for duties cycles between 60% and 90%. In particular this region is of interest for the model because we can obtain the equilibrium average voltage of the coil in this range. The resulting curve is shown in Fig. 9.

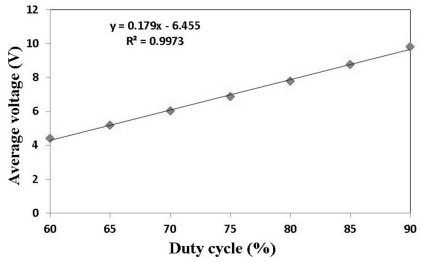

Figure 9: Duty cycle (%) vs Average voltage in the coil terminals (V)

Based on the linear regression obtained in Fig. 9 we can get the parameter P, which is the slope of this linear function, for duty cycles given from 0 to 1 instead of 0% to 100%. Therefore, $P = 17.9$.

The power gain is given in (23).

$$G_p = \frac{1000}{4950} P = 3.62 \tag{23}$$

4. PID Tuning Through Routh Hurwitz's Criterion

With all the values defined above, we have almost completely described the system. However, in order to achieve the magnetic levitation we must find the PID controller's values which stabilize the system. Using the Fig. 5

and the experimental values described in the last section, we can obtain the transfer function in closed loop of the whole system. The unknown values are the proportional, derivative and integral constants of the PID controller. These values can be foundusing the Routh Hurwitz's criterion. All this mathematical analysis and the one of section 2 was done in Maple 12, a CAD tool that allows us to deal easily with complex algebraic expressions. The system transfer function in closed loop is shown in (24).

$$G_{lc} = \frac{-956.4(K_d s^2 + K_p s + K_i)}{s^4 + 98.2s^3 - (1532.2 - 1.82 \cdot 10^6 K_d)s^2 - (1.5 \cdot 10^5 - 1.82 \cdot 10^6 K_p)s + 1.82 \cdot 10^6 K_i} \tag{24}$$

To apply the Routh Hurwitz's criterion it is needed to analyze the characteristic equation of the system which is the denominator of the system transfer function in closed loop equaled zero. This is shown in (25).

$$s^4 + 98.2s^3 - (1532.2 - 1.82 \cdot 10^6 K_d)s^2 - (1.5 \cdot 10^5 - 1.82 \cdot 10^6 K_p)s + 1.82 \cdot 10^6 K_i = 0 \tag{25}$$

From this relation, and applying the Routh Hurwitz's criterion we obtain three mathematical conditions which must be simultaneously satisfied to stabilize the system. These are shown in (26), (27) and (28).

$$0 < 1.82 \cdot 10^6 K_d - 18509.3 K_p \tag{26}$$

$$0 < -2.73 \cdot 10^{11} K_d + 3.3 \cdot 10^{12} K_d K_p + 2.78 \cdot 10^9 K_p - 3.36 \cdot 10^{10} K_p^2 - 1.78 \cdot 10^8 K_i \tag{27}$$

$$0 < 1.82 \cdot 10^6 K_i \tag{28}$$

From (28),K_i must be positive. We can achieve the three values using (26) like a condition to evaluate one variable given the another, and evaluating (27) for a given positive value of K_i . Three values that satisfy (26), (27) and (28) are: $K_p = 1$, $K_d = 0.06$ and $K_i = 2$. These values don't optimize the transient response but stabilize the magnetic levitation system. The optimization will be done by defining certain design specifications for the controller.

4.1. PID discrete controller

The PID controller was implemented digitally, but the whole system was modeled as a continuous system. The discrete approximation for the PID controller can be obtained taking the Z transform of (15). This is shown in (29).

$$U(z) = E(z)K_p \left[1 + \frac{T}{T_i(1 - z^{-1})} + T_d \frac{1 - z^{-1}}{T}\right] \tag{29}$$

Based on (29), the discrete PID controller was implemented in the parallel form. The PID discrete controller's algorithm was written in C and compiled

with CCS compiler, which is a powerful tool for accessing device hardware features from the C language level. Finally the program was recorded within a microcontroller PIC18F2550 from Microchip. It was designed a method to easily reprogram the microcontroller. The approximation of the discrete system as a continuous system will be valid if the sampling time is small enoughtomaintain the dynamic characteristics of the PID continuous controller even though digitalization. From the state of the art [11] was observed that a sampling time of less than 12 ms is suitable.

4.2. Design specifications

Given (26), (27) and (28) we can obtain three constants in a range of possible values which satisfy certain requirements of the transient response. The transient response can be described in function of two factors: response speed and the proximity to the desired values. Based on the physical characteristics of the Electromagnetic Suspension System and a quick desired stabilization were defined the following design specifications:

- A rise time lower than 0.3 s, and a peak time lower than 0.6 s, in order to achieve a fast response of the system.
- An imaginary part for each root of lower 250 rad, to reduce the oscillation in the transient response.
- Magnetic levitation achievable in different equilibrium positions.
- A maximum overshoot of 0.0012 m, in order to avoid that the sphere leaves the operation range of the position sensors.
- A settling time lower than 1 s, time in which the sphere position doesn't change more than 0.0003 m around the equilibrium position.

For a unit-step input of 0.0116 m these requirements were accomplished for the PID constants $K_p = 0.51$, $K_d = 0.02$ and $K_i = 2.3$. In Fig. 10 is shown the step response position and the current intensity through the coil for a reference position input of 0.0116 m. Fig. 10 was obtained by simulating the system in closed loop in Matlab/Simulink. Matlab/Simulink allowed us to see quickly the system's response when one or more parameters were changed.

5. Real implementation

The functional Electromagnetic Suspension System is shown in Fig. 11.

The sampling time used was 1.276 ms. This value includes an expected sampling time of 1 ms plus a delay of 0.276 ms due to the computations within the microcontroller. The levitation was obtained for an equilibrium position of 0.0112 m and an average current through the coil of 1.06 A. The current expected from the modeling was from 1.067 A, which gives a percentual error of 0.7%. The position voltage of the sphere through time is shown in Fig. 12.

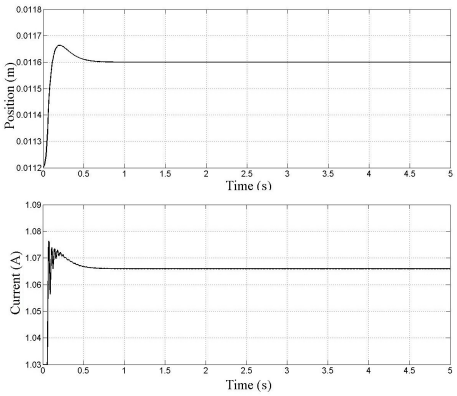

Figure 10: Position and current response for a unit-step of 0.0116 m

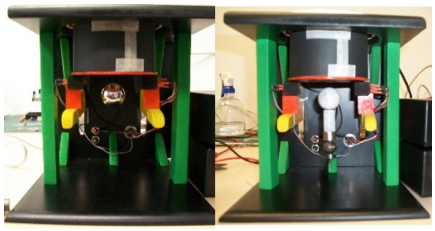

Figure 11: Electromagnetic suspension system

The sphere moves around 0.3 V which is the equivalent to a position of 0.0116 m. A rise time of 0.05 s (lower than 0.3 s) and a peak time of 0.25 s (lower than 0.6 s) were achieved. The overshoot obtained was of 0.0012 m approximately, which accomplishes in the limit with the controller's design requirements. The settling time obtained was of 0.5 s (lower than 1 s). Also levitation was achieved for different equilibrium positions. Experimental measures like that in Fig. 12 and 13 were taken with a digital FLUKE oscilloscope of 40 MHz of band width.

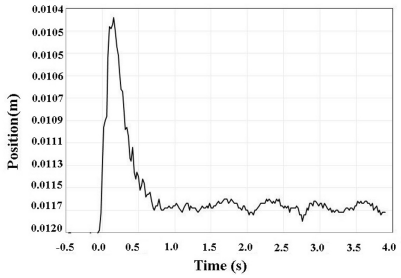

Figure 12: Position voltage output of the magnetic suspension system

An oscillation experiment was made in order to probe the natural frequency of the system predicted by the model. Fig. 13 shows the experimental oscillation of the system. The oscillation frequency measured was about 5.88 Hz for an average period of 0.17 s (see Fig. 13), while the oscillation frequency predicted by the model was 5.9 Hz (the natural frequency shown in (6)).

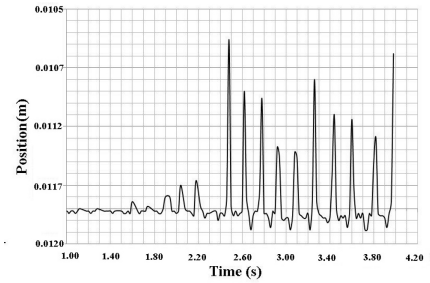

Figure 13: Natural frequency of the system

5.1. Robustness of the system

Several experiments were carried out on the Magnetic Suspension System changing the parameters and observing the system's response. The parameters changed were the object geometry, mass and material. It was observed that the levitation was possible only when the object had a circular profile. This is not weird, because the sensor gain was obtained for an object with circular profile (sphere). For our surprise the levitation was achieved for all those objects (with a circular profile), even though the object properties changed the whole

mathematical model. Also all the operational conditions were changed. The current needed to levitate objects with bigger mass was greater. For objects with the same mass but different shapes the current changed visibly. In Fig. 11, right hand image shows the levitation of a configuration of bodies with different properties. It is notable that a circular profile is only needed in the sensed area, while the attached suspended objects can have any shape.

6. Conclusion

It was designed a magnetic suspension system from an inter-disciplinary point of view: physics and mathematical modeling, electronic and mechanical design, control and systems design. The mathematical construction was used to predict suitable values of the PID controller constants. These values were used in the real implementation of the discrete PID controller to achieve stable levitation, and accomplishing with certain design specifications defined previously. The robustness of the PID controller designed is evident experimentally. Several experiments were carried out in order to achieve a stable levitation even though the uncertain when each parameter (equilibrium voltage, equilibrium position, mass, geometry, materials, shape) was changed. Successfully the levitation was achieved in all those experiments.

Parameters such as sampling time, the sensor's curve, power gain are very important in order to define a compact system. It was guaranteed that each parameter was maintained constant even when uncertain appeared, in order to achieve reproducibility in the experiment.

This work can give new and fresh ideas in order to carry out researching in more complex and advanced magneticssystems. These ideas are concerned with the integration of tools coming from different areas, including conceptual design applied in the whole system design methodology.

References

[1] H. W., G., Electromagnetic design of a magnetic suspension system, IEEE Transactions on education 40 (1997) 30–35.

[2] S. L., Z. K., K. B., An electromagnetic launcher with magnetic levitation realized based on vector control, IEEE transactions on magnetics 45 (2009) 467–470.

[3] P. A., V. J., E. J., van, Magnetic levitation systems compared to conventional bearing systems, Microelectronic Engineering ELSEVIER 83 (2006) 1372–1375.

[4] S. C., M. N., P. B., Maglev apparatus for power minimization and control of artificial hearts, IEEE transaction on control system technology 16 (2008) 13–18.

[5] W. M. A., W. D. L., M. H. J., S. G. M., Magnetic levitation of helium liquid, Low temperature physics 106 (1997) 50–58.

[6] K. B., K. N., N. T., Performance improvement of a magnetically levitated microrobot using an adaptive control, Proceeding of the international conference on MEMS, NANO and Smart systems 23 (2003) 46–52.

[7] K. D., C. W., Integrated monitoring scheme for a maglev guideway using multiplexed FBG sensor arrays, NDT&E International ELSEVIER 42 (2009) 260–266.

[8] Q. K., X. H., Gyro-effect and Earnshays Theorem: Stable and Unstable Equilibrium for Rotatory and Stationary Permanent Magnetic Levitators, in: The 2nd International conference in bioinformatics and biomedical engineering, 1323–1325, 2009.

[9] F. A., C. K., S. D., Electric Machinery, McGrawHill, 2003.

[10] H. W., G., PWM Control of a Magnetic Suspension System, IEEE Transactions on education 47 (2004) 165–173.

[11] Magnetic Levitation System, Feedback Instruments Ltd, 2001.